MOLECULAR DYNAMICS INVESTIGATION OF THE EFFECT OF THE INTERATOMIC POTENTIAL ON STEADY-STATE CRACK PROPAGATION

C. J. Kimmer, J.A. Zimmerman, P.A. Klein, and Er-Ping Chen

ABSTRACT

We present molecular dynamics simulations examining the effect of the interatomic potential on steady-state mode I crack propagation in a two-dimensional triangular lattice as a function of applied strain. The interatomic potential is the Morse potential whose failure strain exhibits linear variation with its exponential parameter. The limiting crack speed is defined to be the steady-state crack velocity observed at the onset of instability in steady-state crack propagation leading to dislocation nucleation or crack branching. For all systems studied, the limiting crack speed is observed to be less than one third the Rayleigh wave speed. The fastest crack propagation in these ideal systems is associated with a material's long-wavelength elastic properties being dominated by the strength of the nearest-neighbor bond.

Key Words: molecular dynamics, crack propagation, dynamic fracture.

I. INTRODUCTION

Brittle fracture is a paradigmatic problem for multiscale modeling because atomic-scale interactions at the crack tip can exert a profound influence on the observed macroscopic crack propagation. Similarly, brittle fracture of ideal, defect-free materials still presents a stringent test for models of crack propagation which typically predict a maximum crack velocity, v_{lim}, of the Rayleigh wavespeed, c_R. Experimentally observed crack speeds are often considerably less than those predicted by existing theories (Ravi-Chandar and Knauss, 1984; Fineberg, *et al*., 1992), and molecular dynamics simulations of ideal materials also often reveal a considerably reduced maximum velocity relative to the continuum predictions (Abraham, 1996; Zimmerman, *et al*., 2002). A complete understanding of brittle fracture in discrete materials is necessary to highlight the material properties determining steady-state crack propagation and to lead to the creation of more accurate continuum models of crack propagation.

Analytic solutions for steady-state crack propagation are available for a range of lattices in two dimensions with nearest-neighbor Hooke's law interactions terminating abruptly at a specified failure separation (Slepyan, 1982; Marder and Gross, 1995). In general, atoms interacting via Hooke's law obtain higher crack velocities than those with more realistic, i.e. nonlinear and softening, interatomic interactions. Molecular dynamics (MD) has been a powerful tool for investigating material response for these nonlinear interactions, although most simulations have been carried out at higher strain rates than the corresponding experimental measurements in order to reduce the computation time.

Holland and Marder report results for Si (1998) crystals at much lower strain rates, corresponding to adiabatic straining where the strain rate is small enough to not perturb the crack tip as displacement waves are generated by the changing boundary conditions. They determine that strain rates $\dot{\varepsilon}$ satisfying $\dot{\varepsilon} << c_s/h$ are adiabatic, with c_s the sound speed and h the system size in the direction of loading.

*Corresponding author. (Email: epchen@sandia.gov)

C. C. Chen is with the Department of Electrical Engineering, National Huwei Institute of Technology, Yunlin, Taiwan 632, R.O.C.

T. L. Chien is with the Graduate School of Engineering Science & Technology, National Yunlin University of Science & Technology, Yunlin, Taiwan 640, R.O.C.

C. T. Wu is with the Department of Electrical Engineering, National Yunlin University of Science & Technology, Yunlin, Taiwan 640, R.O.C.

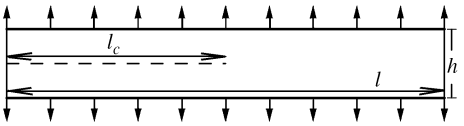

Fig. 1 The system geometry used in this study. The top and bottom three rows of atoms are subject to a constant strain rate. The precrack (dotted line) passes symmetrically between two rows of atoms displaced horizontally by $a/2$ relative to each other

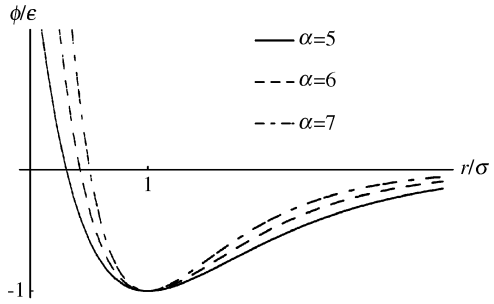

Fig. 2 Variation in the shape of the interatomic potential for α=5 (solid line), 6 (dashed line), and 7 (dotted and dashed line). As α increases, the nearest-neighbor bond stiffness increases while the strain to bond failure decreases

These simulations reveal that the steady-state crack velocity may depend on the loading history (in contrast to the analytic Hooke's law solutions), and that the steady-state velocity versus strain curve may be qualitatively different from available analytic solutions for linear materials.

MD simulations by Abraham (1996) varied the interatomic potential to investigate the maximum attainable crack velocity while Holian and Ravelo (1998) examined the crack velocity and brittle to ductile transition as a function of the potential. Abraham showed that significantly higher crack speeds were obtainable by tailoring the large-strain behavior to be much closer to that of a linear isotropic material. Large-strain isotropic response was achieved by constraining third and fourth-order elastic constants to be zero rather than constraining these moduli to satisfy a more general relationship guaranteeing isotropy. Consequently, these modifications to the interatomic potential are difficult to extend to longer-ranged interatomic interactions where the contributions of bonds from different neighbor shells must be balanced. Recently, Buehler, *et al.* (2003) used a bilinear potential to investigate the effects of both softening and stiffening interactions and found that the hyperelastic response near the crack tip was crucial in determining the crack velocity if the hyperelastic region approaches a characteristic length scale.

Most continuum theories of dynamic crack propagation are in general unsuitable for predicting these atomistic results since the continuum theories depend only on the material's linear elastic properties. Gao (1996) has proposed an explanation for the slow limiting speeds in terms of the hyperelastic response near the crack tip by assuming an equibiaxial stress state at the crack tip. This model provides an explanation for branching instabilities for $v_{lim}/c_R<2/3$, but is less predictive when applied to MD simulations of crack growth (Zimmerman, *et al.*, 2002). The validity of the assumption of an equibiaxial stress state at cohesive failure has not been examined.

II. METHODOLOGY

The ideal material investigated here is a 2D triangular lattice in strip geometry (Fig. 1). The mass m and lattice constant a are both set to unity, and atoms interact as far away as their third nearest neighbors via the Morse potential

$$\phi(r;\ \alpha,\ \sigma,\ \varepsilon)=\varepsilon(e^{-2\alpha(r/\sigma-1)}-2e^{-\alpha(r/\sigma-1)}).$$

The length scale σ is determined from the constraint a=1 for stress-free material. The potential energy well depth ε is arbitrary in the sense that the crack velocity in units of the Rayleigh wavespeed, v/c_R, is independent of ε. By varying α, the shape of the interatomic potentials (Fig. 2) and elastic properties change in a controlled way. The failure strain for a nearest-neighbor bond is inversely proportional to α, so that potentials with larger α are effectively shorter-ranged. Since the lattice is triangular with pair-potential interactions, the long wavelength linear elastic properties are isotropic with one independent elastic modulus, proportional to α^2. Normalizing crack velocities by cR, which is proportional to α, renders results that are independent of the linear elastic properties of the material, although the surface energy also changes with α. However; it is not well understood how this variation may affect the maximum steady-state crack velocity.

The effect of variation in α of the material properties may be stated in terms of the third-order elastic constants. In general, these elastic constants for the 2D triangular lattice do not satisfy the isotropy condition $C_{111}/5C_{112}$=1 (Thurston and Brugger, 1964; Wallace, 1972), and for Morse potentials in the triangular lattice this ratio is a decreasing nonlinear function of α as the relative strengths of bonds with different neighbor shells change with variation in the potential. This ratio provides a quantitative description of how the material response of the system changes with α, and it is useful as a benchmark for comparing different potentials in the same geometry. Nevertheless, its utility is ultimately limited since no models for crack propagation are formulated in terms

of higher-order elastic theory. More qualitatively, larger α corresponds to shorter-ranged interactions in materials with less softening in the nearest-neighbor bond as it is stretched. It is worthwhile to point out that this isotropy ratio is independent of α and equal to 11/5 for nearest-neighbor Morse potentials on a triangular lattice. Consequently, higher-order elastic constants are more useful for characterizing the large strain bulk response of a sample (compare to Abraham, 1996) than characterizing the effects of the interatomic potential on bond softening, particularly at the crack tip.

To study crack propagation as a function of the interatomic potential, the upper and lower three rows of atoms are loaded at a prescribed uniform strain rate. A precrack is introduced in the material by restricting the interaction of atoms across the crack line for $x<l_c$, $l_c=l/2$. For the systems studied here, we take $l=150\ a$ and $h=138\sqrt{3}/2a$. Incremental increases in the applied strain followed by energy minimizations are used to determine the Griffith strain, ε_G, for which a cleaved system is energetically favored over a strained one with a precrack. From these initial conditions, atoms near the crack tip are given small velocities and constant strain rates are applied to the top and bottom three rows. After a small induction time, the crack tip is in equilibrium with the loading waves, and the crack velocity may be followed as a function of the applied strain. All strains will be measured in terms of $\Delta\equiv\varepsilon_{yy}/\varepsilon_G$; the strain rate used is $\dot{\Delta}=10^{-6}\ c_s/h$. Simulation results have been verified to be independent of the choice of time step, system size, and strain rate.

To obtain long cracks with a minimum of simulation time, "conveyor belt" boundary conditions (Holland and Marder, 1998) on the left and right sides are used to "paste" new atoms in strained material ahead of the crack tip from atoms in the wake of the crack tip. These boundary conditions mimic a strip of infinite length, for which the moving crack evolves towards steady-state propagation. For the system studied here, a typical simulation box contains ~21,000 atoms at any given time but models a system containing many more distinct atoms; the crack length at the end of a simulation is typically two orders of magnitude larger than the simulation box length. Finally, ramped damping is applied on the left and right sides to reduce wave reflection at the boundary. Values of α used in this study range from 5.0 to 7.0. Smaller values of α result in ductile materials with rapid dislocation nucleation upon application of strain (Holian and Ravelo, 1998) and are not suitable for these simulation methods.

III. RESULTS

The adiabatic crack velocity as a function of strain is shown in Fig. 3. These curves differ markedly from the corresponding ones for linear materials, but are qualitatively similar to ones obtained using a Lennard-Jones potential (Marder, private communication). Similarly, low limiting speeds have been observed before in MD simulations using the Lennard-Jones potential in the same geometry at higher strain rates (Zimmerman, *et al.*, 2002). This same study revealed that increasing the range of the interatomic potential decreases the steady-state crack velocity. The most striking features of the curves in Fig. 3 are the velocity "plateaus" with little change in crack velocity over a range of strains. Such plateaus have been seen before in MD simulations of Si crystals (Holland and Marder, 1998), and are not an artifact of the time step chosen or strain rates used. The strain at which one plateau transitions to another does depend on the loading history; in particular, the abrupt transition at a given strain is not always reversible.

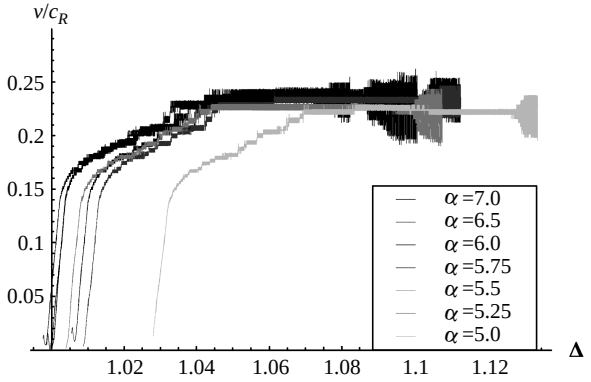

Fig. 3 The normalized crack velocity for the third-nearest neighbor Morse potentials as a function of dimensionless strain, Δ

The large oscillations in v in Fig. 3 begin at strains in which steady-state crack propagation is no longer stable. This micro-cracking instability arises in the triangular lattice as crack-tip bonds parallel to the direction of crack propagation become stretched to failure as the strain increases (Marder and Gross, 1995). At the strain rate used to produce Fig. 3, the crack continues to propagate along the mid-line of the system; at strain rates 100 times larger, dislocation emission along with crack propagation off this line of symmetry is observed. For this work, we concentrate on the plateau with maximum crack velocity before the large oscillations and instability are observed (Fig. 4); we equate this maximum plateau velocity with a steady-state limiting velocity. This plateau is the one occupying the greatest range of applied strains, and over this range of strains the energy emitted by the crack tip in the form of phonons increases with strain. Although the absolute change

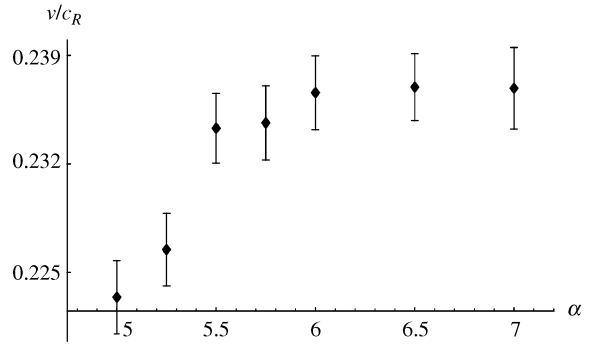

Fig. 4 Limiting velocity as a function of interatomic potential. Velocities and error bars are obtained by averaging over the final plateau in each potential's v vs. Δ curve

in limiting velocity is small between the smallest and largest values of α used, the different limiting velocities are resolved quite well by this simulation method. There is a clear trend of increasing limiting velocity with α that levels off as α increases and the steeper potential well reduces the effect of long-range interactions.

To study the effect of the range of the potential, the same simulations are repeated for Morse-potential interactions cut off just beyond the nearest-neighbor bond length. For these interactions, steady-state crack propagation at speeds above .25 c_R is observed for all values of α, strengthening the contention that the primary effect of increasing α in the third nearest-neighbor systems is to reduce the influence of shells of more distant neighbors. The constant ratio $C_{111}/5C_{112}$ for the nearest-neighbor case indicates that isotropic elastic response at long wavelengths does not correlate with observed limiting crack velocities.

Estimates of the limiting crack velocities shown in Fig. 4 using Gao's theory do not agree well with these simulation results. The limiting velocities are overestimated by 31% at α=7 and 46% at α=5, and the predicted trend of decreasing limiting velocity with α does not agree with the simulation results. It is interesting to note that the predictions of Gao's theory using the nearest-neighbor Morse potential agree with the trend seen here, although the limiting speed for all α is consistently overestimated by ~40%. For these two different choices of the interaction cutoff for the Morse potential, the critical stretch determining the limiting speed using Gao's theory is virtually independent of the range of the potential; however, the Rayleigh wavespeed is much more strongly dependent on the relative strengths of the further- and nearest- neighbor bonds.

A description in terms of long wavelength elastic properties and a description in terms of the effective elastic moduli in Gao's theory differ in their treatment of the dispersion relation. The Rayleigh wavespeeds and elastic moduli C_{111} and C_{112} take the undeformed crystal as the reference configuration; the effect of large strains near the crack tip is manifest in the terms of order ε_{ij}^3 and higher in the long-wavelength expansion of the crystal's potential energy. Gao's theory takes into account the effects of strain at the crack tip on the dispersion relation by determining the limiting speed from the effective elastic moduli B. The variation in limiting velocities with α indicate the importance of nonlinear elastic effects on the crack velocity, so that Gao's assumption of an equibiaxial stress state at cohesive failure should be examined. The simulations presented here are ideal for investigating how the crack-tip state at instability varies with the interatomic interaction, and this is a subject of ongoing study.

IV. CONCLUSION

Adiabatic crack velocities for a wide range of strains have been given for a set of tailored interatomic interactions. It is seen that the fastest crack propagation corresponds to both a greater range of Hooke's law behavior in agreement with Abraham (1996) and to a reduced range of interatomic interaction. These two effects are not separable in this study or in a description in terms of long-wavelength elastic properties. Similarly, the materials with the most pronounced softening are observed to have the slowest crack velocities.

This study is useful in showing a broad range of steady-state crack velocities in ideal brittle materials and illustrating the strong effects nonlinear elastic response can have on crack propagation. These effects are often not incorporated into continuum models of dynamic fracture, but it is apparent that they must be considered for even the simplest model materials.

ACKNOWLEDGMENTS

The authors acknowledge productive and interesting discussions with Michael Marder, who also provided the conveyor belt code. This work was performed at Sandia National Laboratories, California. Sandia is a multiprogram laboratory operated by Sandia Corporation, a Lockheed Martin Company, for the United States Department of Energy's National Nuclear Security Administration under Contract DE-AC04-94AL85000.

REFERENCES

Abraham, F. F., 1996, "Dynamics of Brittle Fracture with Variable Elasticity," *Physical Review Letters*, Vol. 77, No. 5, pp. 869-872.

Buehler, M. J., Abraham, F. F., and Gao, H., 2003,

"Hyperelasticity Governs Dynamic Fracture at a Critical Length Scale," Nature, Vol. 426, No. 6963, pp. 141-146.

Fineburg, J., Gross, S. P., Marder, M., and Swinney, H. L., 1992, "Instability in the propagation of fast cracks," *Physical Review B*, Vol. 45, No. 10, pp. 5146-5154.

Gao, H., 1996, "A Theory of Local Limiting Speed in Dynamic Fracture," *The Journal of the Mechanics and Physics of Solids*, Vol. 44, No. 9, pp. 1453-1474.

Holian, B. L., Blumenfeld, R., and Gumbsch, P., 1997, "An Einstein Model of Brittle Crack Propagation," *Physical Review Letters*, Vol. 78, No. 1, pp. 78-81.

Holian, B. L., and Ravelo, R., 1998, "Fracture Simulations Using Large-Scale Molecular Dynamics," *Physical Review B*, Vol. 51, No. 17, pp. 11,275-11,288.

Holland, D., and Marder, M., 1998, "Ideal Brittle Fracture of Silicon Studied with Molecular Dynamics," *Physical Review Letters*, Vol. 80, No. 4, pp. 746-749.

Marder, M., and Gross, S., 1995, "Origin of Crack Tip Instabilities," *The Journal of the Mechanics and Physics of Solids*, Vol. 43, No. 1, pp. 1-48.

Ravi-Chandar, K., and Knauss, W. G., 1984, "An Experimental Investigation into Dynamic Fracture: III. On Steady State Propagation and Branching," *International Journal of Fracture*, Vol. 26, No. 1, pp. 141-154.

Slepyan, L., 1982, "Dynamics of a Crack in a Lattice," *Soviet Physics, Doklady*, Vol. 26, No. 5, pp. 538-540.

Thurston, R. N., and Brugger, K., 1964, "Third-Order Elastic Constants and the Velocity of Small Amplitude Elastic Waves in Homogeneously Stressed Media," *Physical Review*, Vol. 133, No. 6A, pp. A1604-A1610.

Wallace, D. C., 1972, *Thermodynamics of Crystals*, Dover Publications, Mineola, New York, USA, p. 104.

Zimmerman, J. A., Klein, P. A., Chen, E. P., Hwang, R. Q., Hamilton, J. C., Houston, J. E., and Foiles, S. M., 2002, *Crack Nucleation and Growth: Combined Validated Atomistic and Continuum Modeling*, Sandia National Laboratories, Sandia Report SAND2002-8008.

Manuscript Received: Dec. 31, 2002
Revision Received: Jul. 14, 2003
and Accepted: Sep. 26, 2003